Diffusion of the Diboron Pair in Silicon

Gyeong S. Hwang* and William A. Goddard III†
Materials and Process Simulation Center, Beckman Institute (139-74), California Institute of Technology, Pasadena, California 91125
(Received 18 September 2001; published 15 July 2002)

We propose a novel mechanism for the diffusion of a diboron pair in Si, based on first principles density functional theory. We find a reaction pathway along which the boron pair diffuses from one lowest energy configuration of $[\text{B-B}]_s$-$\langle 001\rangle$ to an equivalent structure at an adjacent equivalent site through three local minimum states denoted as $[\text{B-B}]_s$-$\langle 111\rangle$, B_s-B_i, and B_s-B_s-Si_i. The activation energy for the diffusion is estimated to be 1.81 eV in the generalized gradient approximation. A kinetic model suggests that the diboron diffusion plays an important role in determining diffusion profiles during *ultrashallow* junction processing (which requires high boron-dopant concentration as well as high annealing temperature).

DOI: 10.1103/PhysRevLett.89.055901 PACS numbers: 66.30.Jt, 31.15.Ar, 85.40.Ry

As the gate length of semiconductor devices decreases to the diffusion length of dopants by transient enhanced diffusion (TED), it becomes crucial to achieve a precise control of diffusion profiles during implantation as well as postimplantation thermal treatment. Ion implantation followed by thermal annealing is currently the most widely used method for semiconductor doping. This has led to extensive recent investigations into diffusion mechanisms of dopants [1,2]. However, many questions remain unresolved, particularly on the fundamentals of boron diffusion and clustering at high doping levels ($> 10^{18}$ cm^{-3}) inherent to ultrashallow *pn* junction fabrication in Si.

Boron is a major *p*-type dopant in silicon-based devices. It has been thought that the boron substitution-Si interstitial pair, (B_s-Si_i), is mainly responsible for B TED [2,3] via the so-called "kick-out" mechanism [4,5] or the direct interstitial hopping mechanism [6,7]. However (vide infra), the TED mechanism does not explain the concentration-dependent diffusion observed at high B concentrations ($> 10^{18}$ cm^{-3}) during high temperature annealing ($\approx 1200\,^\circ$C) where B clustering is insignificant [8]. Here B diffusion is enhanced with B concentration, leading to *shouldering* in diffusion profiles [9]. Thus, there must be some other mechanism that significantly facilitates TED at high concentration.

For high concentrations, a mobile B_s-Si_i species may be captured by a second B complex to form a stable multiboron cluster. Such clustering impedes B TED substantially. For instance, upon annealing 600 °C, B TED is noticeable only at $<10^{18}$ cm^{-3}, where cluster formation is insignificant. In this case, the displacement of diffusion profiles becomes larger as the B concentration decreases, exhibiting a *tailing* behavior [10]. Given the tendency of increased retardation by clustering at higher concentration, we consider it is unlikely that B_s-Si_i diffusion is responsible for the anomalous shouldering, suggesting that there must exist some other diffusing component.

Based on a kinetic model, Vandenbossche and Baccus [11] showed that including a mobile and inactive substitutional-interstitial boron cluster (B_s-B_i) gave the best agreement with the experimental results of Inada *et al.* [12]. However, based on *ab initio* density functional theory (DFT) studies Zhu *et al.* [5] claimed that "*B_s-B_i is (relatively) immobile; it is impossible to find a migration path that only breaks one or two bonds while still keeping two B atoms together.*" Consequently, diboron diffusion has been neglected in more recent theoretical studies [13].

Using *ab initio* DFT we have reexamined the diffusion of the diboron (B_s-B_i) pair in Si. We find a new mechanism for diffusion of a boron pair that leads to a total energy barrier of 1.81 eV. Using a kinetic model we show below that when the B concentration and annealing temperature are both very high the contribution of B_s-B_i diffusion can be comparable to or exceed that of B_s-Si_i diffusion. Indeed this mechanism leads to rates that explain the observed shoulder in TED. Our new mechanism involves diffusion of the dimer from one lowest energy [B-B]-$\langle 001\rangle$ configuration to another equivalent configuration through three local minimum states: [B-B]-$\langle 111\rangle$, B_s-B_i, and B_s-B_s-Si_i. We find that the energy barriers for jumping from one local minimum structure to another are each less than 1.0 eV, suggesting that the boron pair can easily change configuration at high temperatures.

All atomic structures (Fig. 1) were optimized using the local density approximation (LDA) [14] to DFT, as implemented in the CPMD V3.3 package [15]. Then at the optimum structure (either a minimum or a saddle point), we evaluated the energy using the generalized gradient approximation (GGA) [16]. The LDA and GGA values are virtually identical as shown in Fig. 2 so that we present only the GGA numbers in the text. These calculations used a nonlocal, norm-conserving pseudopotential [17] and a plane-wave cutoff energy of 20 Ry. The defect systems considered in this study were modeled using a 192-atom supercell with a fixed volume that yields a Si-Si bond distance of 2.35 Å in pure Si. All atomic positions were allowed to relax fully until all residual forces were smaller than 5×10^{-4} Hartree/Bohr. Because of the large supercell, we use just one k point at Γ for the Brillouin-zone (BZ) integrations.

 © 2002 The American Physical Society

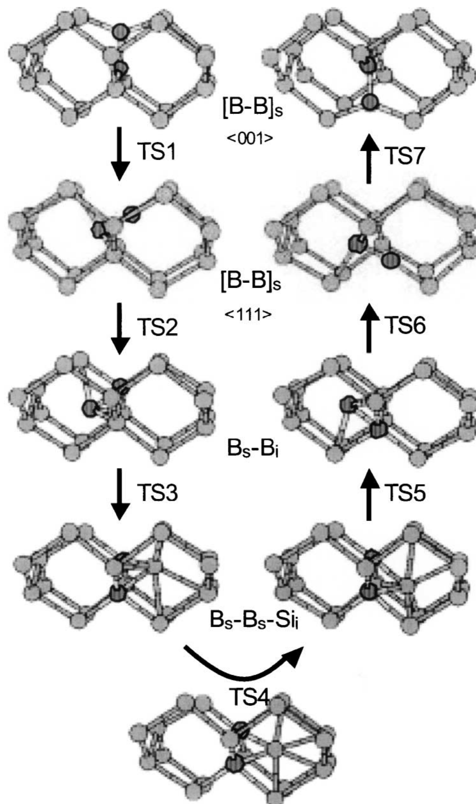

FIG. 1. The pathway for boron dimer diffusion in Si.

Figure 1 shows the structures along the pathway for diffusion of a boron-boron pair in Si. This involves four stable states: (i) $(B\text{-}B)_s\text{-}\langle 001\rangle$, (ii) $(B\text{-}B)_s\text{-}\langle 111\rangle$, (iii) $B_s\text{-}B_i$, and (iv) $B_s\text{-}B_s\text{-}Si_i$ (with optimized atomic structures presented in Fig. 3).

Here $(B\text{-}B)_s\text{-}\langle 001\rangle$ is the lowest energy configuration. As shown in more detail in Fig. 3(a), it has a normal 1.597 Å B-B single bond with each B forming a normal 2.00 Å bond to two Si atoms. In addition, each B has the ideal sp^2 planar bonding configurations while each neighboring Si is essentially tetrahedral.

In the first transition state (TS1), the lower B atom (denoted B_b) moves to the left along a $\langle 110\rangle$ direction while pushing the upper B atom (denoted B_a) in the opposite direction. This leads to the $(B\text{-}B)_s\text{-}\langle 111\rangle$ structure in Fig. 3(b) in which B_b forms normal 2.05 Å bonds to three Si, while B_a forms a compressed 1.94 Å bond to one Si and a compressed 1.56 Å donor-acceptor bond to B_b. Again the two B atoms are bonded to share a single lattice site but are now displaced along a $\langle 111\rangle$ direction.

The second transition state (TS2) involves displacement of the B dimer along the $\langle 111\rangle$ direction away from the Si bonded to B_a. This leads to the $B_s\text{-}B_i$ state in which B_a has normal to long bonds (2.08, 2.23, 2.23, and 2.29 Å) with all four Si atoms, making it a B_s, while B_b has a normal bond 1.65 Å to the B_s and long bonds ($\sim$2.24 Å) to three of the Si, making it a B_i. One can visualize the bonding here in terms of B_s as B^- and B_i as B^+. Here, the bond between B_a and the upper layer Si atom, broken during the first step, is restored.

Next, B_b kicks into a lower layer Si site and the kicked-out Si atom (denote Si_c) moves into an interstitial position along a $\langle 111\rangle$ direction, leading to the $B_s\text{-}B_s\text{-}Si_i$ state. The third transition state (TS3) shows that the adjacent Si, originally bonded to Si_c, simultaneously forms bonds with B_b. The result is that both boron atoms become substitutional (think of them as B^-) while Si_c is displaced to an interstitial site (think of it as Si^{2+}). The $B_s\text{-}B_s\text{-}Si_i$ state leaves the B-B bond broken (2.231 Å compared to 1.60). However, two B atoms remain strongly connected (at 1.956 and 2.203 Å) through the Si interstitial, Si_c, but with the Si atom bonded more strongly to the kicked-in B atom. In addition to the two B, Si_c has bonds to four other

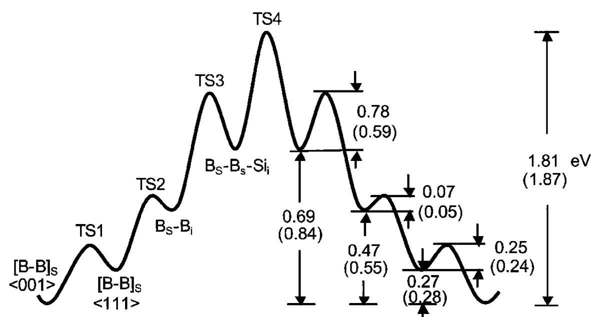

FIG. 2. Energetics (DFT/GGA in eV) along the reaction pathway for boron dimer diffusion in Si. LDA results are in parentheses.

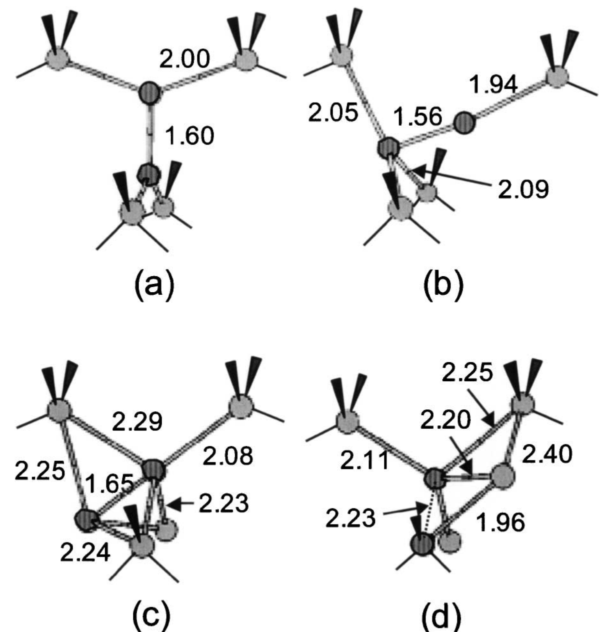

FIG. 3. Structures for minima along the reaction pathway for boron dimer diffusion in Si. (a) $[B\text{-}B]_s\text{-}\langle 001\rangle$, (b) $[B\text{-}B]_s\text{-}\langle 111\rangle$, (c) $B_s\text{-}B_i$, (d) $B_s\text{-}B_s\text{-}Si_i$.

Si [2.40 Å shown in Fig. 3(d) and 2.532.59 Å to others]. Thus, it is in the $\langle 111 \rangle$ direction from B_b.

Next, the Si interstitial (Si_c) jumps down to become an interstitial in the $\langle 11\text{-}1 \rangle$ direction from B_a, leading to a new equivalent B_s-B_s-Si_i state. This involves the fourth transition state (TS4).

Next, we continue through TS5 (equivalent to TS3) but with Si_c displacing B_a to the interstitial position. Then TS6 (equivalent to TS2) with B_a bonding to three Si atoms and B_b bonding to B_a and one Si. Finally TS7 (equivalent to TS1) takes us to another lowest energy configuration, $[B\text{-}B]_s$-$\langle 001 \rangle$, but displaced in the $\langle -1\,1\,-1 \rangle$ direction from the original. Simultaneously Si_c has moved in the $\langle 1\,-1\,1 \rangle$ direction.

Energetics.—Figure 2 presents the potential diagram for the boron-pair diffusion. There are four energy barriers along the diffusion pathway. The first barrier (TS1) from [B-B]-$\langle 001 \rangle$ to [B-B]-$\langle 111 \rangle$ is estimated to be 0.52 eV in LDA (GGA). The [B-B]-$\langle 111 \rangle$ configuration is less stable than the [B-B]-$\langle 001 \rangle$ configuration by 0.27 eV, but the barrier of 0.25 eV for returning back to the $[B\text{-}B]_s$-$\langle 001 \rangle$ state implies that the $[B\text{-}B]_s$-$\langle 111 \rangle$ configuration could be stable even at high temperatures.

The second barrier (TS2) from $[B\text{-}B]_s$-$\langle 111 \rangle$ to B_s-B_i is 0.27 eV, while the formation energy difference between the two configurations is 0.20 eV. Thus with a return barrier of only 0.07 eV, this state is probably not stable.

Next, TS3, the kick-in of the B interstitial into the lower layer Si site requires a rather large energy barrier of 1.00 eV. Here the B_s-B_s-Si_i configuration is stabilized with a sizable barrier of 0.78 eV, for the reverse jump, suggesting that this state might also be stable.

Since the energy barriers for jumping across these local minimum structures are ≤ 1.0 eV, we expect that the B-B pair easily switches its configuration from $[B\text{-}B]_s$-$\langle 111 \rangle$ to B_s-B_s-Si_i at high temperatures.

TS4 leads an energy barrier of 1.12 eV. Thus, assuming steady state kinetics, the overall activation energy required for boron pair diffusion is estimated to be 1.81 eV (the largest barrier). This energy barrier is far smaller than the value 3.5 eV generally quoted for B_s diffusion [18]. We see below that the diboron pair is an important diffusing component responsible for boron TED.

Role in dopant profiling.—We first estimate the diffusivity of B_s-B_i:

$$D_m = D_0 \exp(-E_m/k_B T),$$

where D_0 is the prefactor and E_m is the diffusion energy barrier. The Debye frequency of Si ($\nu_D \approx 10^{13}$ sec^{-1}) and a jump distance of $\delta \approx 2.5$ Å suggest $D_0 = \nu_D \delta^2/6 \approx 1 \times 10^{-3}$ cm^2/sec. This leads to a diffusivity of 3.8×10^{-11} cm^2/sec for $E_m = 1.81$ eV at 1000 °C. This value is about 4 orders of magnitude larger than the value of $D_m(B_s) = 0.757 \times \exp(-3.46/k_B T)$ cm^2/sec $= 5.2 \times 10^{-15}$ cm^2/sec for B_s diffusion [18]. Although the predicted B_s-B_i diffusivity is still far smaller than the B_s-Si_i diffusivity of 1.6×10^{-6} cm^2/sec [for $E_m(B_s\text{-}Si_i) = 0.68$ eV [6]], the larger binding energy for B_s-Si_i [19] leads to a diffusion length for B_s-B_i comparable to that of B_s-Si_i at high temperatures [20].

At low B concentrations, the concentration of the boron dimer, B_s-B_i is quite small, leading to negligible diffusion. However, the B_s-B_i population rises rapidly with the total B density. Using a kinetic model, we have simulated the variation of B_s-Si_i and B_s-B_i concentrations with respect to the total boron concentration. The result is displayed in Fig. 4. In this calculation, we take into account only the formation/dissolution of B_s-Si_i and B_s-B_i pairs; that is, $B_s + Si_i \leftrightarrow B_s\text{-}Si_i$ and $B_s + B_s\text{-}Si_i \leftrightarrow B_s + B_i \leftrightarrow B_s\text{-}B_i$. This neglects many details in the interactions between B and Si atoms, but such simplified kinetics should give a reasonable description in the overall physical picture, especially for variations in the concentration. As the total boron concentration is increased, the concentration of B_s-B_i pairs increases *almost quadratically*. In contrast, B_s-Si_i increases *sublinearly* at high concentration region due to suppression by B_s-B_i clustering. That is, the mobile B_s-Si_i species is more quickly captured by the increased B_s to produce B_s-B_i. At 10^{20} cm^{-3}, the equilibrium concentrations of B_s-B_i are predicted to be 2.2×10^{19} while B_s-Si_i is 1.7×10^{15} cm^{-3}, the B_s-B_i concentration is 4 orders of magnitude larger than the B_s-Si_i concentration.

Based on the equilibrium concentrations (C_{eq}) and the diffusivities (D_m), we can compare the contributions of B_s-B_i and B_s-Si_i to B TED:

$$2D_m(B_s\text{-}B_i)C_{eq}(B_s\text{-}B_i)/D_m(B_s\text{-}Si_i)C_{eq}(B_s\text{-}Si_i),$$

where the factor of 2 arises since two boron atoms are

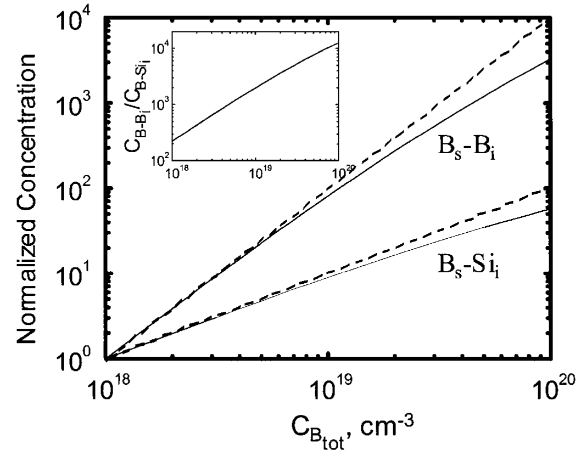

FIG. 4. Normalized concentrations (with respect to $C_{B_s\text{-}B_i}$ and $C_{B_s\text{-}Si_i}$ at $C_{B_{tot}} = 10^{18}$ cm^{-3}) of B_s-B_i and B_s-Si_i as a function of the total B concentration ($C_{B_{tot}}$). The inset shows the concentration ratio between B_s-B_i and B_s-Si_i. In this calculation, the concentration of single Si interstitials and the temperature are kept at 1×10^{14} cm^{-3} and 1000 °C, respectively.

carried upon B_s-B_i diffusion. For 10^{20} cm^{-3}, the relative contribution of B_s-B_i is estimated to be 0.4–0.6 at 1000 °C, but it drops rapidly as the B concentration and/or the temperature decreases. This indicates that the B_s-B_i component should be as important as the B_s-Si_i pair in determining diffusion profiles when both B concentration and annealing temperature are very high.

In addition to Vandenbossche and Baccus's work [11], the role of B_s-B_i diffusion can also be inferred from the observation of anomalous shouldering in diffusion profiles [9]. Clearly, such behavior cannot be explained by B_s-Si_i diffusion alone. If B_s-Si_i diffusion were dominant, the diffusion profile would evolve into a "tailed shape" due to increased trapping of B_s-Si_i at higher concentration. Alternatively it would have a "Gaussian shape" for single component diffusion (in the absence of trapping). On the other hand, since the B_s-B_i concentration increases almost *quadratically* with B concentration, B TED appears to be facilitated at higher concentration when B_s-B_i diffusion becomes important [9]. Given that such shouldering is observed only during high temperature annealing at the region of high B concentrations, we conclude that B_s-B_i diffusion plays a key role in defining the diffusion profiles.

In conclusion, from first principles DFT calculations we have identified a favorable diffusion pathway for the diboron pair in Si. The diffusion energy barrier is estimated to be 1.81 eV in GGA. A kinetic model suggests that a B_s-B_i pair becomes an important diffusing component when both boron-dopant concentration and annealing temperature are very high.

We thank Masamitsu Uehara and Yuzuru Sato of Seiko-Epson for suggesting this problem and providing many helpful discussions. We thank Seiko-Epson for providing financial support. The facilities of the MSC are also supported by grants from DOE-ASCI, ARO/DURIP, ARO/MURI, NIH, Chevron-Texaco, Beckman Institute, 3M, Dow Chemical, Avery-Dennison, Kellogg's, and Asahi Chemical.

*Current address: Department of Chemical Engineering, University of Texas at Austin, Austin, TX.

†To whom correspondence should be addressed.
Email address: wag@wag.caltech.edu

[1] P.M. Fahey *et al.*, Rev. Mod. Phys. **61**, 289 (1989).

[2] A. Ural *et al.*, J. Appl. Phys. **85**, 6440 (1999), and references therein.

[3] N.E.B. Cowern *et al.*, Phys. Rev. Lett. **67**, 212 (1991).

[4] G.D. Watkins, in *Radiation Damage in Semiconductors*, edited by P. Baruch (Dunod, Paris, 1965), p. 97; C.S. Nicholas *et al.*, Phys. Rev. B **40**, 5484 (1989).

[5] J. Zhu *et al.*, Phys. Rev. B **54**, 4741 (1996); J. Zhu, Comput. Mater. Sci. **12**, 309 (1998).

[6] B. Sadigh *et al.*, Phys. Rev. Lett. **83**, 4341 (1999).

[7] W. Windl *et al.*, Phys. Rev. Lett. **83**, 4345 (1999).

[8] E. Schroer *et al.*, Appl. Phys. Lett. **74**, 3996 (1999).

[9] G.S. Hwang and W.A. Goddard, III (to be published).

[10] E. Napolitani *et al.*, Appl. Phys. Lett. **75**, 1869 (1999); E.J.H. Collart *et al.*, J. Vac. Sci. Technol. B **18**, 435 (2000).

[11] E. Vandenbossche and B. Baccus, J. Appl. Phys. **73**, 7322 (1993).

[12] T. Inada *et al.*, Appl. Phys. Lett. **58**, 1748 (1991), they performed thermal annealing at 800 °C for 30 min and at 1000 °C for 10 sec after the predeposition step for B concentration of 4×10^{20} cm^{-3} at the surface

[13] L. Pelaz *et al.*, Appl. Phys. Lett. **70**, 2285 (1997); M. Uematsu, J. Appl. Phys. **84**, 4781 (1998); S.K. Theiss *et al.*, Thin Solid Films **365**, 219 (2000).

[14] D.M. Ceperley and B.J. Alder, Phys. Rev. Lett. **45**, 566 (1980); J. Perdew and A. Zunger, Phys. Rev. B **23**, 5048 (1981).

[15] J. Hutter *et al.*, CPMD, MPI fuer Festkoerperforschung and IBM Zurich Research Laboratory, 1995–1999.

[16] J.P. Perdew *et al.*, Phys. Rev. Lett. **77**, 3865 (1996).

[17] S. Goedecker *et al.*, Phys. Rev. B **54**, 1703 (1996).

[18] R.B. Fair, in *Impurity Doping Process in Silicon*, edited by F.F. Yang (North-Holland, Amsterdam, 1981), p. 315.

[19] The binding energy of B_s-B_i tends to be greater than that of B_s-Si_i by about 0.7 eV [5].

[20] The projected diffusion length is given by $\lambda = \sqrt{6D_m/D_{\rm diss}}$, where $D_{\rm diss}$ is the dissociation rate. Since a species must diffuse one jump away from the cluster to be dissociated, for B_s-B_i, the dissociation rate can be simplified as $D_{\rm diss} = \nu_D \exp\{-[E_m(B_s\text{-}Si_i) + E_b(B_s\text{-}B_i)]/k_BT\}$. Taking $D_m(B_s\text{-}B_i) = 0.001 \times \exp(1.84/k_BT)$, $E_m(B_s\text{-}Si_i) = 0.68$ eV [6], and $E_b(B_s\text{-}B_i) = 1.6$ eV [estimated 0.7 eV larger than $E_b(B_s\text{-}Si_i) = 0.9$ eV [6]], we obtain $\lambda = 1.9$ nm at 1000 °C. This value is comparable with the value ≈ 2 nm estimated for B_s-Si_i diffusion [3,6].